

Characterization and diurnal variation of size-resolved inorganic water-soluble ions at a rural background site

Rita Ocskay,^{*a} Imre Salma,^a Wan Wang^b and Willy Maenhaut^b

Received 30th September 2005, Accepted 12th December 2005

First published as an Advance Article on the web 4th January 2006

DOI: 10.1039/b513915e

Water-soluble inorganic ions in aerosol samples have been studied. The sample collection took place during summer in 2003 at a European background site which is operating within the framework of the European Monitoring and Evaluation Program. Gent type PM10 stacked filter unit (SFU) samplers were operated in parallel on a day and night basis to collect particles in separate coarse (2.0–10 μm) and fine (<2.0 μm) size fractions. Particulate masses were measured gravimetrically; the filters from one of the SFU samplers were analyzed by particle-induced X-ray emission spectrometry (PIXE) and instrumental neutron activation analysis (INAA). Filters from the other SFU sampler were analyzed by ion chromatography (IC) for major inorganic anions (MSA^- , NO_2^- , NO_3^- , Cl^- , Br^- , SO_4^{2-} , oxalate) and cations (Na^+ , K^+ , NH_4^+ , Mg^{2+} , Ca^{2+}). The water-soluble inorganic ions measured were responsible for 44% and 16% of the total fine and coarse particulate mass, respectively. In the fine size fraction, the main ionic components were SO_4^{2-} and NH_4^+ accounting for about 90% of fine ionic mass. In the coarse fraction the main ionic components were Ca^{2+} and NO_3^- , followed by SO_4^{2-} . Significant day and night difference in the mass concentrations was observed only for fine NO_3^- . The molar ratios of fine NH_4^+ to SO_4^{2-} indicated their complete neutralization to $(\text{NH}_4)_2\text{SO}_4$. According to the cation-to-anion ratios the coarse particles were alkaline, while the fine particles were slightly acidic or neutral. By comparing the corresponding concentrations obtained from PIXE/INAA and IC, we determined the water-extractable part of the individual species. We also investigated the effect of long-range transported air masses on the local air concentrations, and we found that the air quality of this background monitoring station was affected by regional pollution sources.

Introduction

In recent years, aerosol particles have received growing attention due to their influence on the global radiation budget^{1–3} and to their adverse effects on public health.⁴ Atmospheric particles originate from both natural and anthropogenic sources. They have large range in size from nanometres to several tens of micrometres, and have multi-component chemical composition including inorganic ions, organic substances, crustal matter, elemental carbon and metallic compounds. The water-soluble fraction plays an important role in atmospheric processes. Due to its hygroscopic nature, it can change the size and atmospheric lifetime of aerosol particles with changes in relative humidity. This phenomenon has an effect on both the direct and indirect radiative forcing of particulate matter by changing the scattering properties of the particles and controlling the cloud formation processes.⁵ Furthermore, the ionic composition of the particles determines their acidity influencing the rate of many chemical reactions occurring in the liquid phase and the partitioning of water-

soluble semi-volatile components between the gas and particle phase.⁶ In these processes, fine particles have greater influence because—according to their size—they interact with solar radiation and also provide cloud condensation nuclei. The knowledge of physical and chemical properties of atmospheric aerosols and understanding of their formation processes and sources are required to assess their potential effects on environment and on human health, and subsequently for developing mitigation strategies.

Detailed data on PM characteristics at a wide variety of sites (background, urban and kerbside sites) in Europe can be found in van Dingenen *et al.*,⁷ Putaud *et al.*,⁸ and Querol *et al.*⁹ The PM mass concentrations at background sites are a combination of particles from natural sources as well as pollutants originating from distant industrial and urban areas.¹⁰ According to the comparison between rural background and urban sites made by the above mentioned authors,^{7–9} the PM mass concentrations inside a city also depend on the background level of the region where they are located, so regional as well as local control strategy is needed to reduce outdoor exposure.

The study presented is part of an international research project on rural aerosol, and its aim was to provide a detailed characterisation of the water-soluble inorganic fraction. Our main objectives were to determine the mass concentration of

^a Institute of Chemistry, Eötvös University, P.O. Box 32, H-1518 Budapest, Hungary. E-mail: rita_ocsokay@citromail.hu

^b Institute for Nuclear Sciences, Ghent University, Proeftuinstraat 86, B-9000 Ghent, Belgium

major inorganic ions and their relative contribution to the aerosol mass; to investigate their temporal variation; to study the ion balance in order to determine the acidity of particles; and also to investigate the effect of long-range transported air masses on the particulate mass and ionic composition.

Experimental methods

Sampling location and methods

The field work took place at the continental (rural) background air monitoring station, K-puszta (46°58'N, 19°33'E and 136 m above the mean sea level). The station is operated within the framework of the European Monitoring and Evaluation Program (EMEP). The site is located approximately 80 km SE of Budapest on the Great Hungarian Plain. The largest city nearby (Kecskemét with about 108 000 inhabitants) is situated at a distance of 15 km.

The aerosol samples were collected by Gent-type PM10 stacked filter unit (SFU) sampler.^{11,12} The device has a PM10 inlet and contains two filters, a coarse and a fine filter, in series. The sampler operates at an air flow rate of 17 l min⁻¹; at this flow rate the 50% cut-off aerodynamic diameter (AD) for the coarse filter is 2.0 µm. Consequently, the aerosol particles are collected in a coarse (2.0–10 µm AD) and a fine (<2.0 µm AD) size fraction. Two SFU samplers were operated in parallel: one sampler (SFU(NN)) with two Nuclepore polycarbonate membrane filters (pore sizes 8 and 0.4 µm) as coarse and fine filters, the other (SFU(NT)) with a coarse Nuclepore polycarbonate membrane filter and a Gelman Teflo membrane filter (pore size 2 µm) as a fine filter. All filters had a diameter of 47 mm, and the coarse filters used were Apiezon coated to reduce particle bounce. The inlets of the samplers were placed facing down at a height of 10 m above the ground, and the collection was performed at ambient temperature and pressure. Collection of the samples was carried out from 4 June through 9 July 2003. Until 1 July, the samples were collected for separate daylight periods and nights starting at about 7:00 and 19:00 local time (UTC+2), respectively; afterwards, daily collections were performed starting at about 7:00 local time. A total number of 55 samples (filter pairs) with a 12 h collection time and 8 samples with a 24 h collection time together with 4 field blank samples were taken with each SFU sampler. All filters were placed in plastic Petrislide dishes, kept cold during transportation and stored in a freezer (at -25 °C) until analysis. During the sampling period basic meteorological parameters (temperature, relative humidity, precipitation, wind speed and direction) and ozone concentration were also recorded on hourly basis.

Chemical analyses and data treatment

The PM mass was measured gravimetrically by a microbalance (with a sensitivity of 1 µg) before and after the sampling. Each filter was pre-equilibrated at 25 °C and 50% relative humidity for 24 hours before the actual weighing. The coarse polycarbonate and fine Teflon filters from the SFU(NT) sampler were analyzed by ion chromatography (IC) for major water-soluble inorganic ions using a DIONEX 4500i instrument with a PC-based AutoIon (AI-450) data acquisition and analysis system.

One half of each filter was placed in a 15 ml polystyrene tube and extracted with 5 ml Millipore simplicity water (resistivity > 18 MΩ cm). For the Teflon filters, we followed a three-step extraction: 1 hour ultrasonication, 1 hour mechanical shaking and 30 minute ultrasonication. The polycarbonate filters were only ultrasonicated for 1 hour. For the determination of anions (*i.e.*, methanesulfonate (MSA⁻), NO₂⁻, NO₃⁻, Cl⁻, Br⁻, SO₄²⁻, oxalate), AG12 guard and AS12 analytical columns were used, while cations (*i.e.*, Na⁺, K⁺, NH₄⁺, Mg²⁺, Ca²⁺) were measured by CG12 guard and CS12 analytical columns with ASRS-Ultra and CSRS-Ultra auto-suppressors, respectively, both operating in auto-suppression mode. The elution was performed with 2.7 mM Na₂CO₃/0.3 mM NaHCO₃ for the anions and with 20 mM MSA for the cations with a flow rate of 1 ml min⁻¹ and under isocratic conditions. A conductivity detector was used for the detection. The injection of the extracts was done manually using a 1 ml syringe and through a membrane filter unit with a pore size of 0.22 µm (Millipore Corporation, USA). The volume of the sample loop was 100 µl. To check the quality of the IC measurements analyses and evaluation of standard solutions were performed, and calibration procedure was repeated regularly. Laboratory blanks were processed and analyzed simultaneously with the real samples to monitor the background contamination. The polycarbonate coarse and fine filters from the SFU(NN) sampler were analyzed by particle-induced X-ray emission spectrometry (PIXE)^{13,14} and by instrumental neutron activation analysis (INAA).¹⁵ By combining PIXE and INAA data, we obtained concentrations for up to 46 elements from Na to Th. The quality of the analytical data was continuously controlled on a sample by sample basis through the PIXE/INAA concentration ratios for elements that were measured by both analytical techniques.¹⁶ The IC and PIXE/INAA analyses were carried out at Ghent University.

We calculated the fine-to-coarse and night-to-day mass concentration ratios for PM and ionic components. For the determination of ion balance and acidity of particles, charge equivalent cation-to-anion ratios including all ionic species measured, and molar ratios between ammonium and sulfate and nitrate were calculated. The elemental concentrations derived from the PIXE/INAA analyses were compared to the ionic concentrations obtained from IC. To examine the effect of long-range transported air masses on PM and ionic components, air mass back trajectories were calculated according to the US National Oceanic and Atmospheric Administration's Hybrid Single-Particle Lagrangian Integrated Trajectory model (HYSPPLIT version 4)¹⁷ utilizing the Final Model Run (FNL) meteorological data set. Five-day isentropic backward trajectories were computed for arrival levels of 800, 850 and 925 hPa at 00:00 and 12:00 UTC arrival times for night and daylight periods, respectively. In general, the sampling campaign could be characterized by stable meteorological conditions. The weather was especially warm and dry, and did not change significantly during the campaign. The mean values and standard deviations of temperature were 28.5 ± 3.1 °C and 19.0 ± 3.1 °C, and of relative humidity were 41 ± 10.6% and 76.7 ± 9.5% during days and nights, respectively.

Table 1 Mean PM mass concentrations and standard deviations in $\mu\text{g m}^{-3}$ obtained with the SFU samplers using polycarbonate/polycarbonate (SFU(NN)) and polycarbonate/Teflon (SFU(NT)) filter sets for the fine and coarse size fractions

	Daytime periods		Nights	
	SFU(NT)	SFU(NN)	SFU(NT)	SFU(NN)
PM2.0	14.3 ± 4.2	14.3 ± 4.5	15.1 ± 4.7	13.2 ± 3.9
PM10-2.0	9.5 ± 2.6	9.4 ± 2.5	10.8 ± 4.1	10.8 ± 4.1

Results and discussion

Fine-to-coarse ratios and diurnal variation of PM and inorganic ions

The mean fine and coarse PM mass concentrations (and standard deviations) obtained from the SFU(NN) and SFU(NT) samplers are summarized in Table 1. For the coarse polycarbonate filters, there was practically no difference between the two samplers. The mean coarse PM mass ratios and standard deviations were 1.01 ± 0.09 and 1.00 ± 0.07 for daytime periods and nights, respectively. For the fine size fraction, the mean mass ratios of Teflon filters to polycarbonate filters were 1.06 ± 0.06 and 1.05 ± 0.05 for daytime periods and nights, respectively.

The temporal variations of fine and coarse mass concentrations as obtained from the SFU(NT) sampler are shown in Fig. 1. It shows that the coarse particle mass varied irregularly around its median and no particular trend can be observed. In contrast, the PM2.0 mass concentrations were typically larger than the median during the first half of the campaign (04–19 June), and typically smaller from 20 June on. The mass ratios of the fine size fraction to the coarse size fraction (F/C ratios) varied from 0.39 to 3.1 with a median of 1.41, and had very

weak correlation with PM10 mass, which points to different source types and/or processes for the fine and coarse particles. We found a stronger correlation between PM2.0 and PM10 size fractions ($r = 0.84$) than between PM10-2.0 and PM10 fractions ($r = 0.68$) showing that fine particles were mainly responsible for PM10 temporal variability.

The mean night-to-day (N/D) ratios for the individual mass concentrations were 1.14 and 1.06 in the coarse and fine size fractions, respectively. A possible explanation for the larger night concentrations is the reduction of the boundary layer mixing height that causes enhanced atmospheric concentrations although the source intensities are smaller. On the other hand, during daytime the larger ambient temperature and smaller relative humidity favour the volatilization of semi-volatile species from the fine particles, while they can condense on larger (alkaline) particles at night.

The inorganic water-soluble ions accounted for 44% and 16% of the fine and coarse particulate mass, respectively. Relative contribution of the main inorganic ions to the fine and coarse ionic mass (IM) is shown in Fig. 2. The major components in the fine fraction were: SO_4^{2-} (median: 3400 ng m^{-3}), NH_4^+ (median: 1630 ng m^{-3}) and NO_3^- (median: 270 ng m^{-3}). These secondary inorganic species accounted for about 96% of the fine IM and 39% of the total fine particle mass. In the coarse size fraction, the main water-soluble inorganic ions were Ca^{2+} (median: 560 ng m^{-3}) and NO_3^- (median: 460 ng m^{-3}) followed by SO_4^{2-} (median: 310 ng m^{-3}) and NH_4^+ (median: 100 ng m^{-3}); the minor species (Mg^{2+} , Na^+ , K^+ and Cl^-) accounted for the remaining 11% of coarse IM.

Sulfate and ammonium were present mainly in the fine fraction with median F/C mass ratios of 11.7 and 15.7, respectively. For the typical soil-derived species, *i.e.* Ca^{2+} and Mg^{2+} , the median F/C mass ratios were 0.16, but for

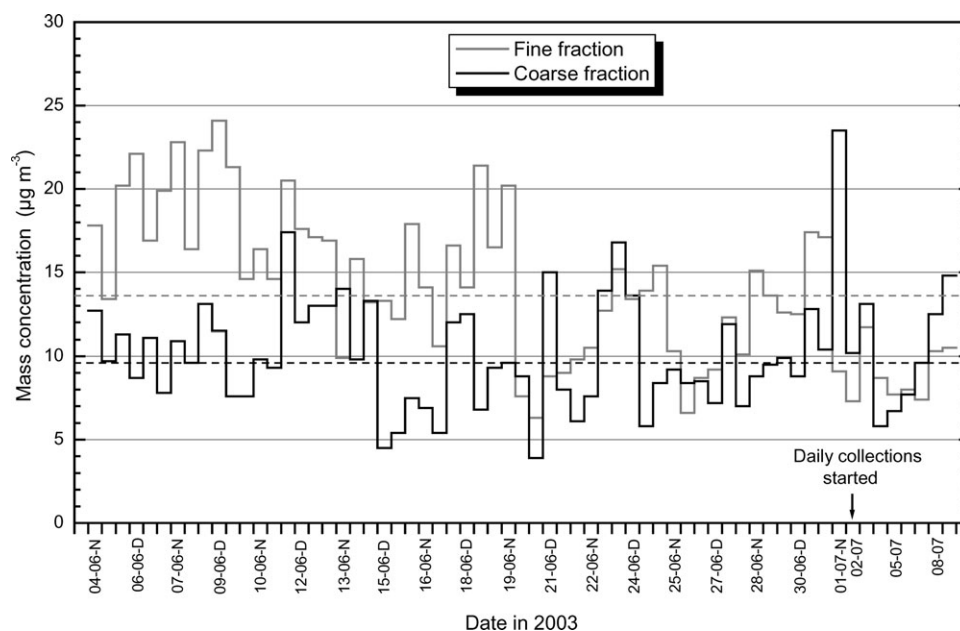


Fig. 1 Temporal variation of aerosol mass concentration. Median values for fine ($13.6 \mu\text{g m}^{-3}$) and coarse size fraction ($9.6 \mu\text{g m}^{-3}$) are represented by dashed lines (D: daytime periods, N: nights).

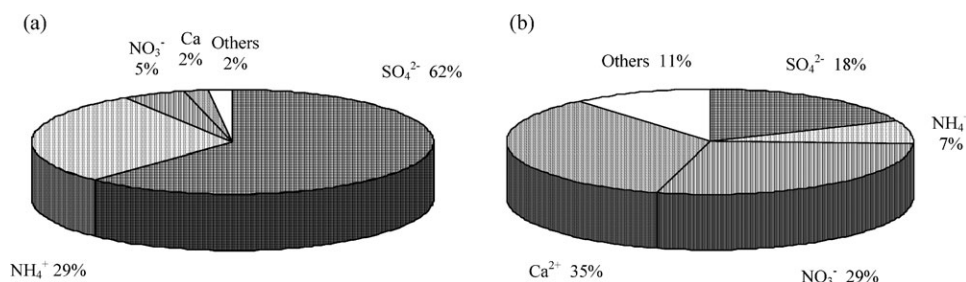


Fig. 2 Relative contribution of main water-soluble inorganic ions to the fine (a) and coarse ionic mass (b). The median ionic mass concentrations were 5.5 and 1.70 $\mu\text{g m}^{-3}$, respectively. Minor components include Na^+ , K^+ , Mg^{2+} and Cl^- .

K^+ the ratio of 1.37 indicated some anthropogenic sources. With regard to nitrate, the median F/C ratio was 0.53 but varied over a wide range from 0.15 to 3.4.

For most ionic species measured, a typical diurnal variation could not be observed. Significant difference in mass concentrations between daytime periods and nights existed only for fine nitrate. The mean N/D mass ratios were 2.9 and 0.95 for the fine and coarse size fractions, respectively. Nitrate in the fine fraction was present most likely as semi-volatile ammonium nitrate, while in the coarse fraction, it was bound to Na^+ and Ca^{2+} (see next section). Variations in the fine nitrate concentration can partially be due to diurnal changes in gas/particulate phase partitioning of NH_4NO_3 and/or in its sampling artefacts which are affected (among others) by ambient temperature and relative humidity. The volatilization of NH_4NO_3 from Teflon membrane filters is a well-documented artefact^{18–20} which can result in underestimated nitrate concentrations especially in summer if not corrected for. The mean N/D mass ratio for sulfate was 0.90 which may suggest that some sulfate was formed locally through photochemical oxidation during daylight periods.

We also examined the dependence of the relative contribution of secondary inorganic species to the PM_{2.0} mass on the source region of the air masses reaching the site. The calculated average concentrations together with the relative contributions characterizing each sampling period were grouped together according to the backward trajectories, and are summarized in Table 2. Changes in PM_{2.0} mass caused by the different type of trajectories can be also followed in Fig. 1. Some typical trajectories are displayed in Fig. 3a–c. The largest PM_{2.0} mass, SO_4^{2-} and NH_4^+ concentrations were observed on the first few days of the campaign (05–09 June) when air masses circulated mainly above the Balkans and the Carpathian Bay for several days (see Fig. 3a). Between 10–25 June the air masses were originated mainly from the Atlantic Ocean. Until 14 June they passed through Western Europe (*i.e.*, Spain, France, Austria), while between 14 and 20 the air

masses mainly arrived through North-Western Europe (Great Britain, Germany, Poland, Czech Republic) (see Fig. 3b). After 14 June the temperature dropped by about 7 °C, on the following days some rain showers also occurred and the relative humidity was much higher than its mean value (50% and 85% during days and nights, respectively). There was no significant difference in the PM_{2.0} mass for these two periods, but the contribution of secondary ionic species to the fine ionic mass was larger in the later case. On 20 June a quickly moving westerly front reached Hungary causing significant decrease in the aerosol concentration. On the subsequent days when air masses travelled above the ocean for about 72 hours before reaching Europe, sea salt in the coarse size fraction could also be observed, while in most part of the campaign its concentration was below or close to the detection limit. Fine particle mass was increasing monotonically after the front until the 25 June when the source region of the air masses was shifted to the Scandinavian region and Northern Europe (see Fig. 3c). Except on a few days between 30 June and 4 July with air masses of westerly origin, the trajectories generally followed the same path till the end of our campaign. Large fine NH_4^+ concentration was observed on those days when air masses came from West Europe and passed over Northern Italy (Po Valley).

The comparison with earlier observations at K-puszta indicates that the aerosol mass concentration has been decreasing in recent years. In 1996 the mean PM_{2.5} mass was 21 $\mu\text{g m}^{-3}$,²¹ and in 1999, Temesi *et al.*²² measured 27 $\mu\text{g m}^{-3}$ in the PM_{2.6} size fraction. With decreasing fine particle mass, the chemical composition of the fine fraction also changed showing increased relative contribution from secondary ionic species. On average, 28% (19% sulfate, 8% ammonium and 1% nitrate) of the PM_{2.5} mass²¹ and 15% (10% sulfate, 4.5% ammonium and 0.4% nitrate) of the PM_{2.6} mass²² was accounted by the secondary ionic species, while the corresponding percentage was 42% (27% sulfate, 13% ammonium and 2% nitrate) in the present study.

Table 2 Mean concentrations of fine particulate mass and secondary inorganic ions (SII) (ng m^{-3}) and their contribution to the PM_{2.0} mass according to the typical source of backward air mass trajectories. Relative contribution for each ion is given in parentheses

Source region	PM _{2.0}	SO_4^{2-}	NH_4^+	NO_3^-	SII/PM _{2.0}
The Balkans, Austria, Carpathian Bay	20.7	6280 (30%)	2860 (14%)	350 (1.7%)	46%
West Europe (Spain, France), Atlantic	15.2	3490 (23%)	1620 (11%)	270 (2.1%)	36%
North-West Europe (Great Britain, Germany), Atlantic	15.7	4270 (27%)	2210 (14%)	540 (3.4%)	45%
Scandinavia, North Sea	10.2	2860 (28%)	1360 (13%)	230 (2.5%)	44%

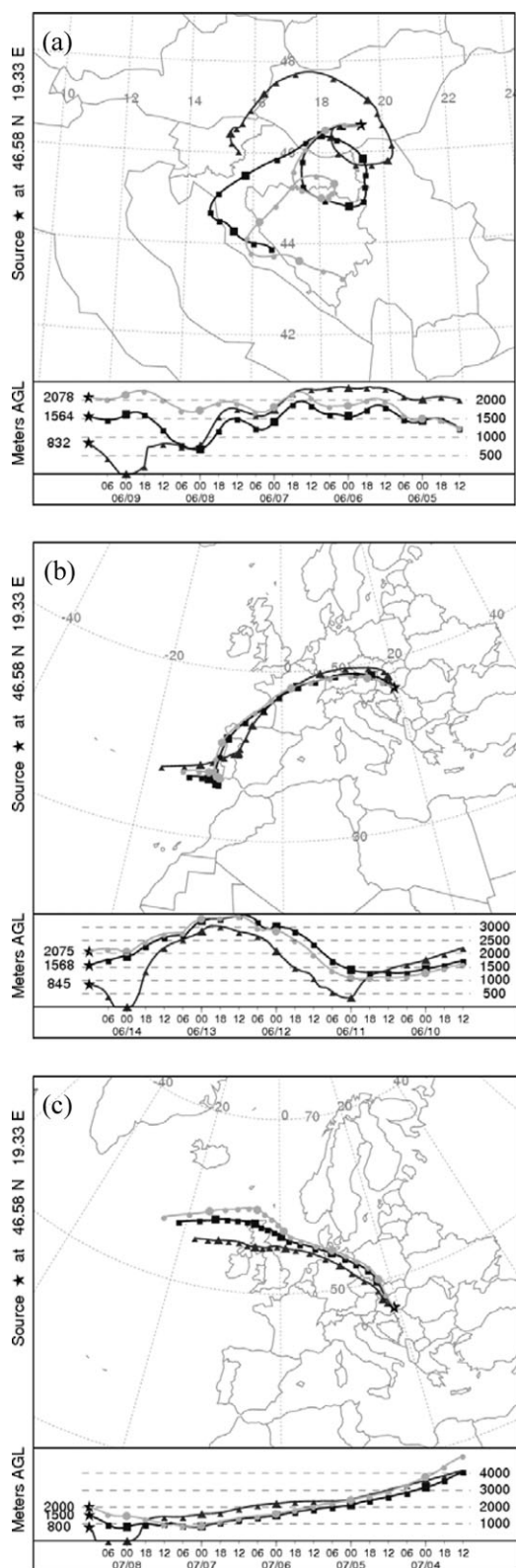


Fig. 3 Some typical examples of backward air trajectories arriving at K-pusztá: 09 June at 12:00 UTC (a), 14 June at 12:00 UTC (b) and 08 July at 12:00 UTC (c).

Table 3 Mean elemental concentrations (SFU(NN) (ng m^{-3}) and mean ionic-to-elemental concentration ratios (SFU(NT)/SFU(NN)) and standard deviations for the fine and coarse size fractions. Number of samples (N) and their correlation coefficient (r) are also shown

	N	SFU(NN)	SFU(NT)/SFU(NN)	r
Fine size fraction				
K	30	81 ± 29	0.51 ± 0.21	0.53
Ca	58	93 ± 46	0.88 ± 0.18	0.89
SO ₄ ^a	63	4443 ± 1771	0.80 ± 0.08	0.97
Coarse size fraction				
Na	49	96 ± 59	0.60 ± 0.21	0.92
K	63	155 ± 62	0.23 ± 0.07	0.71
Mg	45	170 ± 49	0.48 ± 0.12	0.75
Ca	63	556 ± 269	1.01 ± 0.16	0.94
SO ₄ ^a	63	423 ± 149	0.77 ± 0.11	0.94

^a For SFU(NN) samples SO₄ = 3S (see text for more details).

Comparison of elemental and ionic concentrations

The ionic and total (elemental) concentrations of some aerosol components were compared in order to investigate the water solubility of the individual species and also to check the reliability of the applied analytical methods. The two nuclear-related analytical techniques (PIXE and INAA) measure the elemental concentration, while the water-soluble fraction can be obtained from IC. The mean ratios and standard deviations of ionic and elemental concentrations, and the corresponding correlation coefficients are summarized in Table 3. Those species (*i.e.*, Na, Mg, Cl and Br in the fine size fraction, and Cl, Br in the coarse fraction) for which the concentrations were below the detection limit in either analytical technique were excluded from the comparison. We found good correlation between the mass concentrations, especially for Na and Ca. The weak correlation for fine K can be explained by the limited number of data obtained from IC, and by the large analytical uncertainties of the IC data.

About half of the total amount of coarse Na and coarse Mg, and about 80% of coarse K existed in water-insoluble forms. With regard to Ca, the agreement between IC and elemental concentration data indicates that it was totally water-dissolvable. Elemental sulfur was compared to sulfate assuming that S was in the form of SO₄²⁻. Strong correlations between S and SO₄²⁻ concentrations were observed in both fine and coarse fractions (see Table 3) indicating a good consistency in the analytical data. According to the calculations, only (80 ± 8)% and (77 ± 11)% of total fine and coarse SO₄²⁻ was water-soluble. The deviation from 100% is somewhat larger than can be explained by the analytical uncertainty of the analysis methods and suggests that part of the sulfur was present in another form than water-soluble sulfate. Hillamo *et al.*²³ also observed a difference of 10–25% between sulfate derived from PIXE sulfur and sulfate measured by IC similar to our results, but Graham *et al.*²⁴ reported much larger differences.

Ion balance

Cation-to-anion ratios. For the measured cations (Na⁺, K⁺, NH₄⁺, Mg²⁺, Ca²⁺) and anions (MSA⁻, NO₂⁻, NO₃⁻, Cl⁻, Br⁻, SO₄²⁻) charge equivalent cation-to-anion ratios were calculated. The median values of the ratios (and ranges) were

Table 4 Median of molar equivalent ratios (and ranges) of NH_4^+ to SO_4^{2-} and NO_3^- ions in the fine and coarse size fraction

	Fine size fraction		Coarse size fraction	
	Median	Ranges	Median	Ranges
$\text{NH}_4^+/\text{SO}_4^{2-}$	2.5	2.1–4.0	1.90	0.69–3.3
$\text{NH}_4^+/(\text{SO}_4^{2-} + \text{NO}_3^-)$	2.2	1.71–2.5	0.57	0.15–1.52
$\text{NH}_4^+/(2\text{SO}_4^{2-} + \text{NO}_3^-)$	1.19	0.98–1.43	—	—

1.25 (1.06–1.57) and 2.87 (1.46–6.26) in the fine and coarse size fractions, respectively. The possible cause of these large values is the existence of other water-soluble anions not included in our IC analysis. In the case of coarse particles the large cation-to-anion ratios were likely due to carbonates (and perhaps partly to silicates) from soil and mineral dust particles which are mainly present in the coarse size fraction, and associated mostly with calcium and partly with other minor mineral components. The correlation coefficient between Ca^{2+} concentration and anion deficit (calculated as an excess of equivalent positive charge) was 0.99. A similar strong correlation between Ca^{2+} and anion deficit was observed by Bardouki *et al.*²⁵ The likely presence of carbonate indicates that the coarse particles were alkaline. As a consequence of their alkaline nature, these particles are capable to take up semi-volatile species (carboxylic acids, nitric and hydrochloric acids) and it also makes them good sites for heterogeneous reactions of acidic gases like SO_2 and NO_2 .

The anion deficit observed for fine particles was likely caused by water-soluble organic acids, like low molecular weight carboxylic acids and humic-like substances.²⁶ At K-pusztá, Krivácsy *et al.*²⁷ found that water-soluble organic substances dominated over inorganic species in the $\text{PM}_{1.0}$ size fraction, each accounting for about 45 and 34%, respectively.

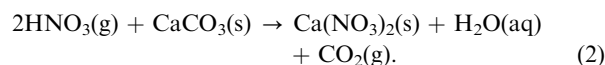
Relationship between ammonium, sulfate and nitrate. The median values and ranges of the equivalent molar ratios of ammonium to sulfate and nitrate are summarized in Table 4. In the fine size fraction, there was a sufficient amount of NH_3 to fully neutralize H_2SO_4 to $(\text{NH}_4)_2\text{SO}_4$. Sulfate in the atmosphere is formed through homogeneous gas phase and heterogeneous gas/particle phase oxidation of SO_2 . The atmospheric lifetime of fine sulfate is in the order of several days,²⁸ so it can be transported far away from its sources during which it interacts with ambient NH_3 . First, partly neutralized and strongly acidic $(\text{NH}_4)\text{HSO}_4$ is formed, which further reacts with NH_3 to produce the weakly acidic $(\text{NH}_4)_2\text{SO}_4$. Aerosol containing mainly $(\text{NH}_4)\text{HSO}_4$ can be considered as moderately aged aerosol, while aerosol containing mainly $(\text{NH}_4)_2\text{SO}_4$ can be viewed as highly aged aerosol.²⁹ Since fine sulfate at our site was present as aged $(\text{NH}_4)_2\text{SO}_4$, it can primarily be associated with long-range transported particles.

Coarse sulfate is present in soil and sea salt particles. Since our sampling site was far from coastal areas, the contribution of sea salt sulfate to the measured sulfate is not expected to be substantial. There was strong correlation between coarse NH_4^+ and both coarse and fine SO_4^{2-} ($r = 0.84$ and 0.79 , respectively), while only a weak correlation was found between coarse SO_4^{2-} and the typical mineral species, Ca^{2+} ($r = 0.04$). Coarse ammonium sulfate was most likely produced by

heterogeneous reaction of NH_3 and H_2SO_4 on the surface of the coarse particles. The equivalent ratio of NH_4^+ to SO_4^{2-} shows that the neutralisation process produced mainly $(\text{NH}_4)\text{HSO}_4$ or a mixture of the two ammonium salts, in contrast to what was the case for the fine particles.

Fine particulate nitrate is formed by homogeneous gas-phase oxidation of nitrogen oxides (NO_x) to gaseous nitric acid, which is followed by the reaction with gaseous ammonia to form highly volatile $(\text{NH}_4)\text{NO}_3$. The distribution of $(\text{NH}_4)\text{NO}_3$ between the gas and particle phases depends mainly upon meteorological conditions (temperature and relative humidity), on the aerosol composition, and on the acidity of the particles. The chemical reaction between sulfuric acid and ammonia is the preferred chemical reaction in the atmosphere.³⁰ As the individual $\text{NH}_4^+/\text{SO}_4^{2-}$ ratios always exceeded 2, an excess amount of ammonia was always present to react with nitric acid. The correlation coefficient between nitrate concentrations and $\text{NH}_4^+/\text{SO}_4^{2-}$ molar ratios was 0.77 showing the effect of H_2SO_4 neutralization on NO_3^- concentration in the particulate phase.

Coarse particulate nitrate can originate from atmospheric reactions of gaseous nitric acid with coarse sea salt and soil particles.³¹



Reaction (1) occurs especially when maritime and polluted continental air masses are mixed. In spite of the inland nature of our sampling site, higher coarse nitrate concentration levels were observed when the air masses originated from the Atlantic Ocean causing elevated sea salt concentration as well.

Summary and conclusions

The water-soluble part of aerosol particles is of great importance, because it determines their bioavailability, their effect on human health, and it also plays an important role in the radiative forcing of particulate matter. Characterisation of particulate matter focusing on water-soluble inorganic ions in aerosol samples collected at a continental background monitoring site in Hungary has been performed and presented in this study. The results show that the fine particulate mass was responsible for the variability of the PM_{10} mass. The anion deficit in the fine size fraction suggested the presence of water-soluble organic acids, while in the coarse fraction the anion deficit was assumed to be attributed to carbonate showing the alkaline nature of the coarse particles which can act as sink for acidic species. Considerable part of fine size fraction contains water-soluble inorganic ions in which the secondary ionic species, *i.e.*, sulfate, ammonium (and nitrate) excessively dominated. Fine sulfate was present as fully neutralized ammonium sulfate which is indicative for aged aerosol. The thorough characterization of the water-soluble inorganic fraction provided by this study can be used as a reference database for monitoring programs in the future.

Acknowledgements

This work was supported by the Hungarian Scientific Research Found (contract number T043348), by a bilateral project between Hungary and Flanders, and by the Belgian Federal Science Policy Office (contact numbers EV/02/11A and BL/02/CR01). We would like to thank J. Cafmeyer for performing the aerosol collection, S. Dunphy for the gravimetric measurements, and N. Raes for the PIXE analyses.

References

- 1 Intergovernmental Panel on Climate Change (IPCC), *Climate Change: The Scientific Basis*, Cambridge University Press, Cambridge, UK, 2001.
- 2 J. E. P. Penner, X. Dong and Y. Chen, *Nature*, 2004, **427**, 231–234.
- 3 P. Crutzen, *Atmos. Environ.*, 2004, **38**, 3539–3540.
- 4 C. A. Pope III, R. T. Burnett, M. J. Thun, E. E. Calle, D. Krewski, K. Ito and G. D. Thurston, *J. Am. Med. Assoc.*, 2002, **287**, 1132–1141.
- 5 M. C. Jacobson, H.-C. Hansson, K. J. Noone and R. J. Charlson, *Rev. Geophys.*, 2000, **38**, 267–294.
- 6 M. Hori, S. Ohta, N. Murao and S. Yamagata, *J. Aerosol Sci.*, 2003, **34**, 419–448.
- 7 R. Van Dingenen, F. Raes, J.-P. Putaud, U. Baltensberger, A. Charron, M.-C. Faccini, S. Decesari, S. Fuzzi, R. Gehrig, H.-C. Hansson, R. M. Harrison, C. Hüglin, A. M. Jones, P. Laj, G. Lorbeer, W. Maenhaut, F. Palmgren, X. Querol, S. Rodriguez, J. Schneider, H. Ten Brink, P. Tunved, K. Tørseth, B. Wehner, E. Weingartner, A. Wiedensohler and P. Wählin, *Atmos. Environ.*, 2004, **38**, 2561–2577.
- 8 J.-P. Putaud, F. Raes, R. Van Dingenen, E. Brüggemann, M.-C. Faccini, S. Decesari, S. Fuzzi, R. Gehrig, C. Hüglin, P. Laj, G. Lorbeer, W. Maenhaut, N. Mihalopoulos, K. Müller, X. Querol, S. Rodriguez, J. Schneider, G. Spindler, H. ten Brink, K. Tørseth and A. Wiedensohler, *Atmos. Environ.*, 2004, **38**, 2579–2595.
- 9 X. Querol, A. Alastuey, C. R. Ruiz, B. Artiñano, H. C. Hansson, R. M. Harrison, E. Buringh, H. M. ten Brink, M. Lutz, P. Bruckmann, P. Straehl and J. Schneider, *Atmos. Environ.*, 2004, **38**, 6547–6555.
- 10 J. C. Chow, J. P. Engelbrecht, J. G. Watson, W. E. Wilson, N. H. Frank and T. Zhu, *Chemosphere*, 2002, **49**, 961–978.
- 11 W. Maenhaut, F. François and J. Cafmeyer, The “Gent” stacked filter unit sampler for the collection of atmospheric aerosols in two size fractions: description and introduction for installation and use, in *Applied Research of Air Pollution Using Nuclear-Related Analytical Techniques*, Report NAHRES-19, International Atomic Energy Agency, Vienna, Austria, 1994.
- 12 P. K. Hopke, Y. Xie, T. Raunemaa, S. Biegalski, S. Landsberger, W. Maenhaut, P. Artaxo and D. Cohen, *Aerosol Sci. Technol.*, 1997, **27**, 726–735.
- 13 W. Maenhaut and H. Raemdonck, *Nucl. Instrum. Methods Phys. Res., Sect. B*, 1984, **1**, 123–136.
- 14 W. Maenhaut, F. François, J. Cafmeyer and O. Okunade, *Nucl. Instrum. Methods Phys. Res., Sect. B*, 1996, **109**, 476–481.
- 15 W. Maenhaut and W. H. Zoller, *J. Radioanal. Nucl. Chem.*, 1977, **37**, 637–650.
- 16 I. Salma, W. Maenhaut, H. J. Annegarn, M. O. Andrea, F. X. Meixner and M. Carstang, *J. Radioanal. Nucl. Chem.*, 1997, **216**, 143–148.
- 17 R. R. Draxler and G. D. Rolph, *HYSPLIT (Hybrid Single-particle Lagrangian Integrated Trajectory) Model*, NOAA ARL READY Website, NOAA Air Resources Laboratory, Silver Spring, MD, 2003, <http://www.arl.noaa.gov/ready/hysplit4.html>.
- 18 C.-J. Tsai and Y.-H. Cheng, *J. Aerosol Sci.*, 1997, **28**, 1553–1567.
- 19 S. Hering and G. Cass, *J. Air Waste Manage.*, 1999, **49**, 725–733.
- 20 M. Schaap, G. Spindler, M. Schulz, W. Maenhaut, A. Berner, W. Wiegprecht, N. Streit, K. Müller, E. Brüggemann, X. Chi, J.-P. Putaud, R. Hitznerberger, H. Puxbaum, U. Baltensberger and H. M. ten Brink, *Atmos. Environ.*, 2004, **38**, 6487–6496.
- 21 A. Molnár, E. Mészáros, H. C. Hansson, H. Karlson, A. Gelencsér, Gy. Kiss and Z. Krivácsy, *Atmos. Environ.*, 1999, **33**, 2745–2750.
- 22 D. Temesi, A. Molnár, E. Mészáros, T. Feckó, A. Gelencsér, Gy. Kiss and Z. Krivácsy, *Atmos. Environ.*, 2001, **35**, 4347–4355.
- 23 R. Hillamo, V. M. Kerminen, M. Aurela, T. Mäkelä, W. Maenhaut and C. Leck, *J. Geophys. Res.*, 2001, **106**, 27555–27571.
- 24 B. Graham, P. Guyon, W. Maenhaut, P. E. Taylor, M. Ebert, S. Matthias-Maser, O. L. Mayol-Bracero, R. H. M. Godoi, P. Artaxo, F. X. Meixner, M. A. Lima Moura, C. H. Eça D’Almeida Rocha, R. Van Grieken, M. M. Glovsky, R. C. Flagan and M. O. Andreae, *J. Geophys. Res.*, 2003, **108**(D24), 4765, doi:10.1029/2003JD004049.
- 25 H. Bardouki, H. Liakakou, C. Economou, J. Sciare, J. Smolík, V. Ždímal, K. Eleftheriadis, M. Lazaridis, C. Dye and N. Mihalopoulos, *Atmos. Environ.*, 2003, **37**, 195–208.
- 26 V. M. Kerminen, R. Hillamo, K. Teinilä, T. Pakkanen, I. Allegrini and R. Sparapani, *Atmos. Environ.*, 2001, **35**, 5255–5265.
- 27 Z. Krivácsy, A. Hoffer, Zs. Sárvari, D. Temesi, U. Baltensberger, S. Nyeki, E. Wiengartner, S. Kleefeld and S. G. Jennings, *Atmos. Environ.*, 2001, **35**, 6231–6244.
- 28 J. H. Seinfeld, *Atmospheric Chemistry and Physics of Air Pollution*, John Wiley & Sons, New York, 1986.
- 29 Y. Hazi, M. S. A. Heikkinen and B. S. Cohen, *Atmos. Environ.*, 2003, **37**, 5403–5413.
- 30 B. H. Baek and V. P. Aneja, and Q. Tong, *Environ. Pollut.*, 2004, **129**, 89–98.
- 31 T. A. Pakkanen, *Atmos. Environ.*, 1996, **30**, 2475–2482.